Mesomorphic Form of Syndiotactic Polystyrene As Composed of Small Imperfect Crystals of the Hexagonal (α) Crystalline Form

Finizia Auriemma, Vittorio Petraccone,* Francesco Dal Poggetto, Claudio De Rosa, Gaetano Guerra, Carla Manfredi, and Paolo Corradini

Dipartimento di Chimica, Università di Napoli Federico II, Via Mezzocannone 4, 80134 Napoli, Italy

Received December 29, 1992; Revised Manuscript Received March 24, 1993

ABSTRACT: An analysis of the structure of the mesomorphic form of syndiotactic polystyrene (s-PS), through Fourier transform calculations on models constituted by large bundles of chains, is presented. Further information on the structural organization in the mesomorphic form is also provided by Fourier transform infrared (FTIR) spectra, in the frequency regions for which well-defined differences exist between the spectra of samples in the α and β crystalline forms. Both theoretical and experimental data provide support for the hypothesis that the mesomorphic form of s-PS contains small and imperfect crystals of the α crystalline form.

Introduction

The synthesis of fully syndiotactic polystyrene (s-PS) has been reported in recent years.[1-3]

Several structural studies, essentially by X-ray diffraction,[4-15] electron diffraction,[16] FTIR,[17-25] and solid-state NMR[26,27] have shown a very complex polymorphic behavior for this polymer. Using the nomenclature proposed in ref 9, this can be described in terms of two crystalline forms, α and β, containing planar zig-zag chains and two others, γ and δ, containing s(2/1)2 helical chains. The general pattern is further complicated by the fact that both the α (hexagonal) and β (orthorhombic) forms can exist in different modifications characterized by differing degrees of structural order, which are intermediate to those of the two limiting disordered modifications (α' and β') and the two limiting ordered modifications (α'' and β''). In these descriptions, structural disorder refers to the positioning of the polymer backbone, while the order in the positioning of the substituent phenyl rings remains unaltered.[4,9,12,14]

Very recently, the presence, for s-PS, also of a mesomorphic form, containing chains in the planar zig-zag conformation[28] (which has been also called the "premature" planar zig-zag form[15]) has been shown.

In our previous contribution on this subject,[29] the XRD pattern of a highly oriented sample of syndiotactic polystyrene in the mesomorphic form, collected by an automatic diffractometer, has been presented, thus providing quantitative information relative to the diffracted intensity. The structural changes induced by annealing procedures in mesomorphic samples have been also described: both unoriented and oriented mesomorphic samples are transformed gradually, into α-form crystals. On the basis of this evidence and of preliminary comparisons between the calculated Fourier transform of simplified models (isolated chains or triplets of chains) and the experimental diffraction intensity, it has been suggested that the local organization in triplets of *trans*-planar chains, typical of the different modifications of the α form, would be largely present also in the disordered chain agglomerates of the mesomorphic form.[29]

In the present contribution a more complete analysis of the structure of the mesomorphic form of s-PS, through Fourier transform calculations on models constituted by large bundles of chains, is presented.

The reported calculations refer mainly to bundles of chains organized as in the α[12] or β[4,14] crystalline forms of s-PS, in which different degrees of paracrystalline disorder are introduced.

In the final section of the paper, further information on the structural organization in the mesomorphic form is obtained by Fourier transform infrared (FTIR) spectra in the frequency regions for which well-defined differences exist between the spectra of samples in the α and β crystalline forms.[21]

Experimental Section

The s-PS ($M_w = 6.6 \times 10^5$ determined by GPC) was supplied by Himont Italia. The polymer fraction insoluble in methyl ethyl ketone is 93%.

Infrared spectra were obtained with a Bruker IFS 66 FTIR spectrometer. The wavenumber range scanned was 4000–400 cm^{-1}. The spectra are reported in absorbance units and are normalized with respect to the band at 1601 cm^{-1}. The reported results were obtained with films 30–50 μm thick. For the preparation of the films the following procedures have been used: amorphous films were obtained by compression molding followed by quenching in a liquid nitrogen bath; mesomorphic films were obtained by annealing amorphous samples at 120 °C for 15 min; films of s-PS in the α crystalline form (α' modification) were obtained by annealing amorphous films at 200 °C; films in the β crystalline form (β' modification) were obtained by compression molding at 330 °C, followed by slow cooling at room temperature.

The fiber X-ray diffraction spectra quoted in this paper are the same as those of ref 29. As described in ref 29, fiber specimens were obtained by strips of quenched films at 105 °C, using a Polymer Lab miniature material tester, at a strain rate of 10 mm/min, with an initial gauge length of 6 mm up to a strain of nearly 6. The X-ray diffraction patterns, with Ni-filtered Cu Kα radiation, were obtained by using a Nonius automatic CAD4 diffractometer (always maintaining an equatorial geometry).

X-ray Diffraction Analysis

The X-ray diffraction spectra of fiber specimens of s-PS in the mesomorphic form (already presented in ref 29) are here partly replotted. The diffraction intensity after subtraction of the background and of the amorphous contribution and after correction by the Lorentz and polarization factors (Lp) (which according to the diffraction geometry is $Lp = (1 + \cos^2 2\Theta)/\sin 2\Theta$) is reported for the equator and for the layer lines with $l = 1$, 2, 3, and 4 in Figure 1A and for the meridian in Figure 2A.

The most important features of the X-ray diffraction spectrum of s-PS in the mesomorphic form can be summarized as follows:

0024-9297/93/2226-3772$04.00/0

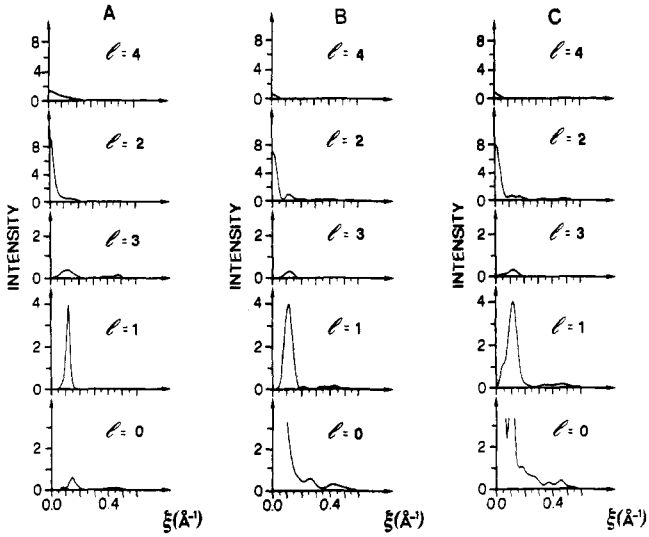

Figure 1. (A) Experimental X-ray diffraction intensity of s-PS in the mesomorphic form for the indicated layer lines (corresponding to a periodicity of c = 5.1 Å), subtracted for the background and the amorphous contribution, hence corrected by the Lorentz and polarization factors. (B) Results of the Fourier transform calculations for the indicated layer lines, for the triplet of s-PS chains in the α form, outlined in Figure 3 by a dashed circle. (C) Results of the Fourier transform calculations for the indicated layer lines, for the triplet of s-PS chains in the β form outlined in Figure 4 by a dashed loop.

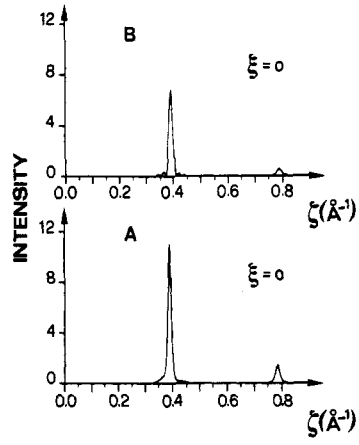

Figure 2. (A) Experimental X-ray diffraction intensity of s-PS in the mesomorphic form on the meridian (ζ = 0), subtracted for the background and the amorphous contribution, hence corrected by the Lorentz and polarization factors. (B) Plot along the meridian of the calculated Fourier transforms presented in Figure 1B,C.

(1) On the equator is a broad peak centered at ξ = 0.14 Å^{-1} spanning between 0.10 Å^{-1} < ξ < 0.18 Å^{-1}.

(2) On the first layer line is a strong diffraction peak with half-width equal to $\Delta\xi$ = 0.03 Å^{-1} centered at ξ = 0.12 Å^{-1}. The ratio between the heights of the two peaks on the first layer line and on the equator is nearly equal to 6.5.

(3) On the third layer line is a diffuse halo centered at ξ = 0.11 Å^{-1}. The ratio between the heights of the two peaks on the third layer line and on the equator is nearly equal to 0.67.

(4) On the second and fourth layer lines are two peaks with maxima located at ξ = 0 (meridional reflections). They are broad along ξ (see Figure 1A) and sharp along ζ (see Figure 2B). The ratio between their heights is about 7.5.

It is worth noting that for polycrystalline uniaxially oriented samples it is not sound to compare quantitatively the so-measured intensities of meridional and nonmeridional reflections. This is due to the difficulty to account for the real portion of matter contributing to the diffraction with varying ξ, for ξ values close to zero. In previous papers this problem was bypassed by considering the intensities integrated over the reciprocal cylindrical coordinate Φ, obtained by multiplying the diffracted intensity by ξ in the approximation of "perfect" c-axis orientation.[30] This procedure, in fact, substantially set at zero the intensities for ξ values close to zero. In this paper we bypass this problem by making quantitative comparisons only between the meridional peaks (on the second and fourth layer lines) or between the nonmeridional peaks (on the equator and the on the first and third layer lines).

Fourier Transform Calculations: Method

In this paper we deal with large bundles of s-PS chains in which "paracrytalline disorder" of the kind discussed by Tadokoro in ref 31 (Chapter 4) is present.

The X-ray diffraction intensity by fibers is conveniently calculated as a function of the reciprocal space cylindrical coordinates ξ, Φ, and ζ as

$$I(\xi,\Phi,\zeta) = F(\xi,\Phi,\zeta)F^*(\xi,\Phi,\zeta) \quad (1)$$

where $F(\xi,\Phi,\zeta)$ is the structure factor and the asterisk denotes the complex conjugate. For the calculation of the diffraction intensity by bundles of chains cylindrically averaged over the reciprocal coordinate Φ, we extend the treatment reported by Tadokoro in ref 31 (Appendix D) for the calculation of the molecular structure factor of nonhelical molecules. Let r_a (r_b), ψ_a (ψ_b), and z_a (z_b) be the cylindrical coordinates of the ath (bth) atom and n the total number of atoms in the structural model; $I(\xi,\Phi,\zeta)$ is evaluated as

$$I(\xi,\Phi,\zeta) = \sum_{b=1}^{n}\sum_{a=1}^{n} f_a f_b \exp\{-2\pi i[\xi r_a \cos(\psi_a - \Phi) - \xi r_b \cos(\psi_b - \Phi) + \zeta(z_a - z_b)]\} \quad (2)$$

In eq 2, f_a and f_b are the atomic scattering factors for ath bth atoms, respectively. The cylindrically averaged diffraction intensity is evaluated by integration of eq 2 over Φ. This is conveniently done as explained in the Appendix, introducing auxiliary variables r_{ab}, representing the distance in the x,y plane between the ath and bth atoms. The result of this integration over Φ from 0 to 2π (dividing the integral by 2π) is

$$I(\xi,\zeta) = \sum_{b=1}^{n}\sum_{a=1}^{n} f_a f_b J_0(2\pi\xi r_{ab}) \exp[-2\pi i\zeta(z_a - z_b)] \quad (3)$$

with $J_0(2\pi\xi r_{ab})$ the zeroth order Bessel's function with argument $2\pi\xi r_{ab}$.

Equation 3 is modified with the introduction of a paracrystalline disorder as explained in the following. For the sake of simplicity, the z cylindrical axis is assumed parallel to the polymer chain axis. We introduce m, the number of atoms within a repeating unit (in our case coinciding with two monomeric units), M, the number of repeating units in a chain, and N, the number of chains (or of triplets of chains) in the considered structural models. The labeling of the atoms is arranged in such a way that a first group of m ($3m$) atoms belongs to a first chain (triplet), a second group of m ($3m$) atoms to a second chain (triplet), and so on. Since the s-PS chains in the structural models taken into consideration are regular, with periodicity c = 5.1 Å, the sums in eq 3 are extended only over the atoms of the repeating unit. We introduce $u_{A\xi}$, $u_{A\zeta}$, $u_{B\xi}$, and $u_{B\zeta}$ the displacements from r_A, z_A, r_B, and z_B, the cylindrical coordinates of the center of gravity of Ath and

Bth chain (triplet), respectively. Equation 3 is rewritten as

$$I(\xi,\zeta) = \sum_{B=1}^{N}\sum_{A=1}^{N}\sum_{b=1}^{km}\sum_{a=1}^{km} f^2 J_0(2\pi\xi r_{AaBb}) \exp[-2\pi i\zeta(z_{Aa} - z_{Bb})] \sin^2(\pi Mc\zeta)/\sin^2(\pi c\zeta) \exp[-2\pi i\xi(u_{A\xi} - u_{B\xi})] \times \exp[-2\pi i\zeta(u_{A\zeta} - u_{B\zeta})] \quad (4)$$

In eq 4 f is the atomic scattering factor of carbon; the term $\sin^2(\pi Mc\zeta)/\sin^2(\pi c\zeta)$ is the square of the Laue factor for a periodic structure along z with period equal to c; r_{AaBb} is the distance in the xy plane between the ath atom belonging to the Ath chain (triplet) and the bth atom belonging to the Bth chain (triplet); $k = 1$ in the case of the sums over a and b extended over the atoms belonging to the single chains, and $k = 3$ in the case of these sums extended over the atoms belonging to triplets of chains.

The introduction of a paracrystalline disorder in our treatment is made as follows. Let us assume that there is no statistical correlation between the individual displacement values ($u_{A\xi}$, $u_{B\xi}$, $u_{A\zeta}$, $u_{B\zeta}$) from the r and z cylindrical coordinates of the centers of gravity of the chains (triplets), due to lattice distortions. The average values of the factors $\exp[-2\pi i\xi(u_{A\xi} - u_{B\xi})]$ and $\exp[-2\pi i\zeta(u_{A\zeta} - u_{B\zeta})]$ over all possible deviations from the cylindrical coordinates of the centers of gravity of the chains (triplets) r and z, following the same treatment used for the calculation of the thermal factor [as reported for instance in ref 32 (Chapter I, pp 22-23)], are $\exp[-2\pi^2\xi^2\langle(u_{A\xi} - u_{B\xi})^2\rangle]$ and $\exp[-2\pi^2\zeta^2\langle(u_{A\zeta} - u_{B\zeta})^2\rangle]$, where the broken brackets indicate the mean value of the squared differences. In the assumption made above that there is no correlation between the displacement values of different chains (triplets), the quantities $\langle(u_{A\xi} - u_{B\xi})^2\rangle$ and $\langle(u_{A\zeta} - u_{B\zeta})^2\rangle$ are taken proportional to the distance in the xy plane between the centers of gravity of the chains (triplets), equal to $u_\xi^2 r_{AB}/r_{12}$ and $u_\zeta^2 r_{AB}/r_{12}$ with r_{12} the projection in the xy plane of the distance vector between the centers of gravity of two first neighboring chains (triplets), r_{AB} the distance in the xy plane between the centers of gravity of the Ath and Bth chain (triplet), and u_ξ^2 and u_ζ^2 the mean square displacements from the coordinates (r and z, respectively) of the centers of gravity of the chains (triplets).

The resulting expression of $I(\xi,\zeta)$ multiplied by the Debye factor

$$D = \exp(-\xi^2 B_\xi/2) \exp(-\zeta^2 B_\zeta/2) \quad (5)$$

with B_ξ and B_ζ the thermal factors along ξ and ζ, respectively, gives eq 6, which is the formula used in our calculation for the diffraction intensity of the bundles:

$$I(\xi,\zeta) = \sum_{B=1}^{N}\sum_{A=1}^{N}\sum_{b=1}^{km}\sum_{a=1}^{km} f^2 J_0(2\pi\xi r_{AaBb}) \exp[-2\pi i\zeta(z_{Aa} - z_{Bb})] D \sin^2(\pi Mc\zeta)/\sin^2(\pi c\zeta) \exp(-2\pi^2\xi^2 u_\xi^2 r_{AB}/r_{12}) \times \exp(-2\pi^2\zeta^2 u_\zeta^2 r_{AB}/r_{12}) \quad (6)$$

In summary in eq 6 are present factors $\exp(-2\pi^2\xi^2 u_\xi^2 r_{AB}/r_{12})$ and $\exp(-2\pi^2\zeta^2 u_\zeta^2 r_{AB}/r_{12})$, which reduce the interference between each couple of chains (triplets)—the more, the higher is their distance in the xy plane. For this reason, in the following, factors $u_\xi^2/r_{12} = U_\xi$ and $u_\zeta^2/r_{12} = U_\zeta$ are referred to as the paracrystalline factors. In particular, setting U_ξ and U_ζ up to 1 gives as result the diffraction intensity of the single chain when $k = 1$ and of a triplet of chains when $k = 3$.

Fourier transform calculations were performed on polymer chains including 10 repeating units, for a total chain length of nearly 50 Å. This value was set on the basis of the experimental half-width of the meridional peaks ($\Delta\zeta \approx 0.017$ Å^{-1}). The chain conformation was set in the minimum conformational energy according to the calculations of ref 33, the chain symmetry being tc. Bundles of chains packed as in the α''[12] and β''[14] forms are considered. For the α' form, statistical disorder exists between two isosteric orientations of the triplets, which leave the positions of phenyl rings nearly unaltered, while the atoms of the polymer backbones are statistically distributed in three positions around the local threefold axes (as discussed in ref 12). Fourier transform calculations are here performed by placing in the corresponding lattice position, with occupation factor $^1/_2$, both of the isosteric triplets.

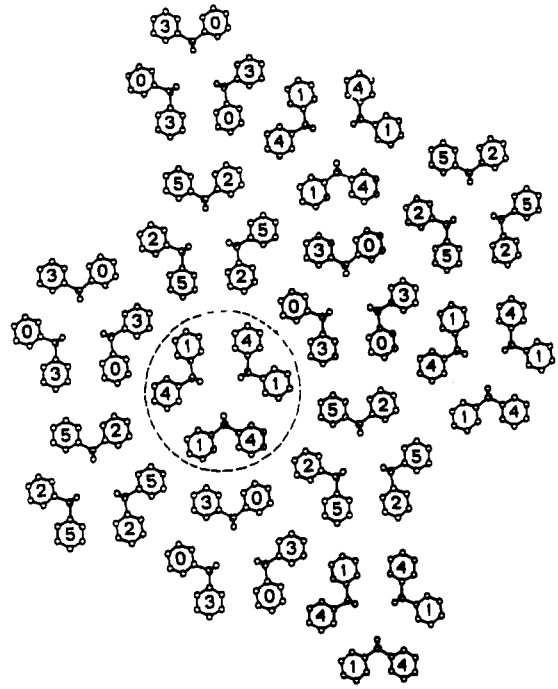

Figure 3. Schematic view in the xy plane of a bundle of 36 chains, packed according to the ordered α'' form.[12] The Fourier transform calculations of Figures 5 and 6 refer to the related disordered α' form (see text). A dashed circle encloses the triplet of chains considered in the calculations of Figure 1B. Relative heights of the centers of the phenyl rings are in units $c/6$.

For the sake of simplicity, in all of the calculations isotropic thermal factors were assumed (B_ξ and B_ζ in eq 5 were placed equal to 8 Å^2). The paracrystalline factors were varied to optimize the agreement with the experimental diffraction data. The calculated X-ray diffraction intensity was evaluated at intervals of $\Delta\xi = 0.005$ Å^{-1} along the layer lines and at intervals of $\Delta\zeta = 0.001$ Å^{-1} along the meridian. To make easier comparisons between the calculated Fourier transform, all of the considered bundles contain an equal number of chains (36 chains).

Fourier Transform Calculations: Results and Discussion

As shown in the previous paper,[29] the experimental diffraction pattern of s-PS in the mesomorphic form (Figure 1A and 2A) can be qualitatively accounted for, at least on the layer lines different from the equator, by the Fourier transform of a triplet of chains placed as in the α crystalline form (Figures 1B and 2B). One of these triplets is pointed out by a dashed circle in the schematic drawing of Figure 3. However, the calculated pattern for this triplet of chains presents a too broad peak on the first layer line and does not account, of course, for the experimentally observed equatorial peak at $\xi = 0.14$ Å^{-1}.

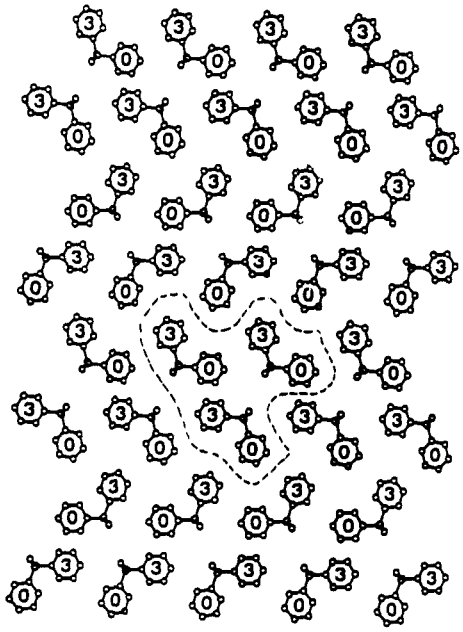

Figure 4. Schematic view in the xy plane of the bundle of 36 chains, packed according to the structure of the β form,[14] used in our Fourier transform calculations of Figure 7. A dashed loop encloses the triplet of chains considered in the calculations of Figure 1C. Relative heights of the centers of the phenyl rings are in units $c/6$.

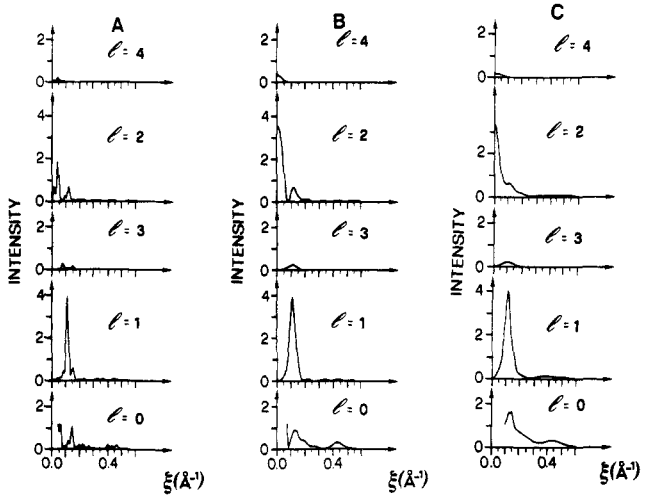

Figure 5. Calculated X-ray diffraction intensity $I(\xi,\zeta)$ vs ξ for the α-form model with placing: (A) $U_\xi = U_\zeta = 0$; (B) $U_\xi = 0.20$ Å, $U_\zeta = 0.033$ Å, $k = 3$ in eq 6 (paracrystalline disorder between the triplets of the kind shown in Figure 3); (C) $U_\xi = 0.20$ Å, $U_\zeta = 0.066$ Å, $k = 1$ in eq 6 (paracrystalline disorder between the chains). Pattern B represents the best agreement reached in the present paper with the experimental pattern of Figure 1A.

Hence, for better agreement with the experimental pattern, Fourier transform of larger bundles of s-PS chains has to be considered. It is worth noting that the Fourier transform of a triplet of chains packed as first neighboring s-PS chains in the β form (for instance, the triplet pointed out by a dashed loop in Figure 4), presents, off the equator, patterns (Figure 1C) similar to the one presented by the α triplet and a meridional pattern essentially identical to that of Figure 2B. Consequently, in our examination of the Fourier transform of large bundles, we start with models in which the chains are packed according to both of the known crystalline forms of s-PS where the polymer chains are in the *all-trans* conformation (the hexagonal α and the orthorombic β forms).

Figure 5 represents the calculated X-ray diffraction intensity $I(\xi,\zeta)$ vs ξ for the α-form bundle (Figure 3) along the equator and the layer lines with $l = 1$, 2, 3, and 4,

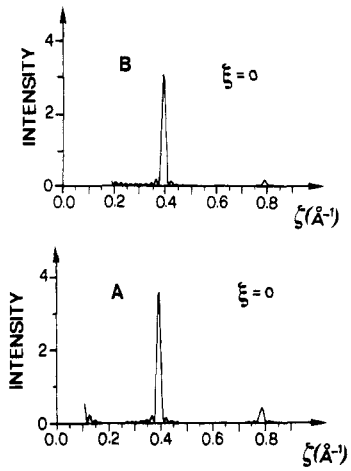

Figure 6. Calculated X-ray diffraction intensity $I(0,\zeta)$ along the meridian for the α model: (A) $U_\zeta = 0.033$ Å, $k = 3$ in eq 6, corresponding to the pattern of Figure 5B; (B) $U_\zeta = 0.066$ Å, $k = 1$ in eq 6, corresponding to the pattern of Figure 5C.

corresponding to the absence of disorder, $U_\xi = U_\zeta = 0$ (Figure 5A), a model with paracrystalline disorder between the triplets of the kind shown in Figure 3 (full order inside the triplets) (Figure 5B), and a model with paracrystalline disorder between the chains (Figure 5C). The results reported for the disordered models correspond to the best found agreement with the experimental data of Figure 1A. In particular, $U_\xi = 0.20$ Å and $U_\zeta = 0.033$ Å for the calculations of Figure 5B, and $U_\xi = 0.20$ Å and $U_\zeta = 0.066$ Å for the calculations of Figure 5C. The plots of the calculated intensity along the meridian $I(0,\zeta)$ vs ζ, corresponding to the pattern of Figure 5B,C are shown in parts A and B, of Figure 6, respectively. The peaks on the second and fourth layer line, which are not meridional in the α form (Figure 5A), become meridional with $U_\zeta \geq 0.026$ Å when $k = 3$ in eq 6 or with $U_\zeta \geq 0.052$ Å when $k = 1$ in eq 6. The narrow peaks of Figure 5A, after introduction of paracrystalline disorder, become broad along ξ, remaining narrow along ζ, and their positions are in good agreement with experimental data (cf. Figure 5B,C with Figure 1A and Figure 6A,B with Figure 2A). As far as the relative intensities are concerned, a better agreement is obtained for the models with paracrystalline disorder between triplets; in particular, the best ratio between the heights of the two peaks on the first layer line and on the equator is about 4 when $k = 3$ in eq 6 and is about 2 when $k = 1$ in eq 6 (as cited before, the experimental value is equal to 6.5). This suggests as more suitable for the mesomorphic form the model with paracrystalline disorder between triplets of chains and complete order inside the triplets, rather than the model with paracrystalline disorder between the chains.

Figure 7 compares the calculated X-ray diffraction intensity $I(\xi,\zeta)$ vs ξ for the β'' bundle (sketched in Figure 4) along the equator and the layer lines with $l = 1$, 2, 3, and 4, for $U_\xi = U_\zeta = 0$ (Figure 7A), and for $U_\xi = 0.20$ Å and $U_\zeta = 0.033$ Å with paracrystalline disorder between the triplets of the kind shown in Figure 4 (Figure 7B). Independently of the setting the value of U_ξ, U_ζ, and k (as well as of B_ξ and B_ζ), some aspects of the calculated patterns remain different from those of the experimental pattern of the mesomorphic form. For instance, not only is the ratio between the heights of the peaks on the first layer line and on the equator always too low (lower than 1.5) with respect to the experimental value but also the maximum of intensity on the equator is located at $\xi = 0.12$ Å^{-1}, while for the experimental pattern it is located at $\xi = 0.14$ Å^{-1}.

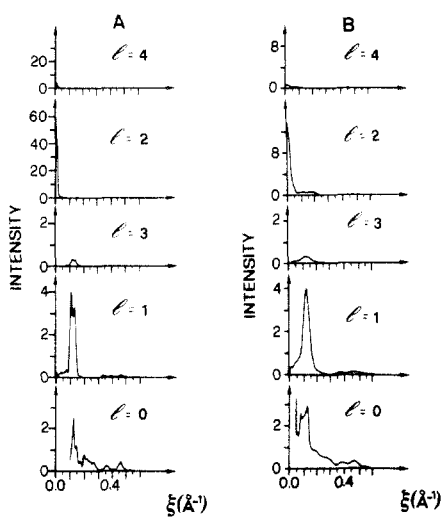

Figure 7. Calculated X-ray diffraction intensity $I(\xi,\zeta)$ vs ξ for the bundle of Figure 4 (β-form model) with placing: (A) $U_\xi = U_\zeta = 0$; (B) $U_\xi = 0.20$ Å, $U_\zeta = 0.033$ Å, $k = 3$ in eq 6.

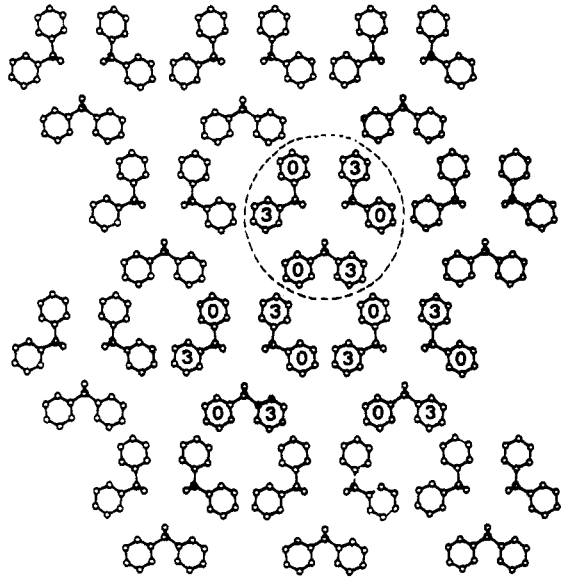

Figure 8. Schematic view in the xy plane of the bundle of 36 chains, packed according to the structure of the α form proposed by Greis et al. in ref 16, used in our Fourier transform calculations of Figure 9. Relative heights of the centers of the phenyl rings are in units $c/6$.

According to other calculations, not reported here, different models presenting disordered arrangements of chains or of triplets of chains (for instance, models showing mixed features of the α and β forms) are not suitable, due to the broadness and low intensity (with respect to the equator) of the peak on the first layer line.

Also, models presenting different ordered organizations of the triplets of chains, typical of the α form, can be unsuitable. Let us consider, for instance, the model of packing of the triplets of Figure 8, which is also energetically feasible.[34] This structure model was proposed for the α form of s-PS[16] and then discarded on the basis of structure factor calculations.[12] Figure 9 shows the calculated $I(\xi,\zeta)$ vs ξ on the equator and the layer lines with $l = 1, 2, 3$, and 4 with U_ξ and U_ζ placed equal to 0 (Figure 9A) and $U_\xi = 0.20$ Å and $U_\zeta = 0.033$ Å, with paracrystalline disorder between the triplets of the kind shown in Figure 8 (Figure 9B). As for the β-form model, the disagreement for the ratio between the intensities on the first layer line and the equator (lower than 2) indicates that this model is less suitable than the model of Figure 5B for representing the mesomorphic form.

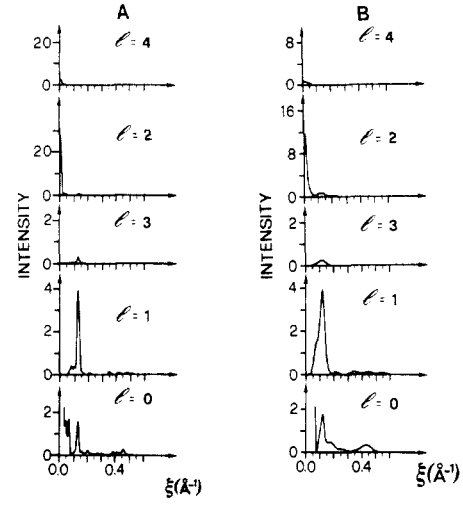

Figure 9. Calculated X-ray diffraction intensity $I(\xi,\zeta)$ vs ξ for the bundle of Figure 8 with placing: (A) $U_\xi = U_\zeta = 0$; (B) $U_\xi = 0.20$ Å, $U_\zeta = 0.033$ Å, $k = 3$ in eq 6.

In summary, the comparison between the Fourier transform calculations and the X-ray diffraction patterns indicates that the mesomorphic form obtained by cold drawing of amorphous s-PS samples is substantially formed by small and imperfect α-form crystals. This comparison suggests also that the disorder is mainly between the triplets of chains, which characterize this hexagonal form.

FTIR Spectra and Packing of the Chains in the Mesomorphic Form

Some Fourier transform infrared data for oriented mesomorphic samples, obtained by using a polarized incident beam and orienting the samples with their stretching axes perpendicular or parallel to the polarization direction, have been reported in ref 28. On the basis of the absorbance of the band at 1222 cm^{-1} (related to the skeletal vibration of chain sequences in *trans*-planar conformations[18,19]), it has been found that the drawing of amorphous samples induces the formation of sequences in *trans*-planar conformation, whose concentration and orientation increase with increasing drawing degree.

Although in the frequency region of the conventionally measured infrared and Raman spectra (400–4000 cm^{-1}) only intramolecular modes appear, some particular bands can be sensitive to intermolecular interactions typical of the different modes of packing of chains with identical conformations. In particular, between the spectra of samples in the α and β crystalline forms of s-PS, well-defined differences exist, although both contain chains in the *trans*-planar conformation.[21] These spectral differences have been shown to be essentially independent of the particular modification obtained (α' or α'', β' or β'') and of the preparative route.[21]

To obtain further information relative to the packing of the chains in the mesomorphic form, the FTIR spectra of unoriented (amorphous, mesomorphic, α form, and β form) samples have been compared in Figure 10 for two particular spectral regions. The spectral region 1110–1400 cm^{-1} (Figure 10A) clearly shows that the mesomorphic sample is definitely different from the amorphous one, mainly for the presence of the band at 1224 cm^{-1}. Moreover, it is apparent that the three main bands in the range 1300–1400 cm^{-1} present, for the mesomorphic form, positions (1335, 1348, 1375 cm^{-1}) and relative absorbances (1.1:1.0:1.0) very close to the positions (1334, 1348, 1375 cm^{-1}) and relative absorbances (1.2:0.8:1.0) of the α form and slightly different from the positions (1337, 1349, 1373

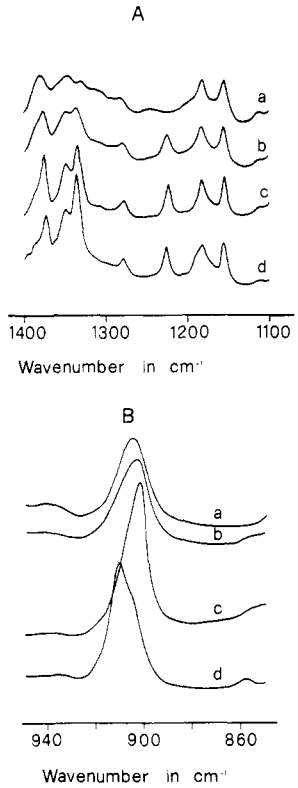

Figure 10. Fourier transform infrared spectra in the spectral regions (A) 1400–1100 and (B) 980–800 cm^{-1} for the samples (a) amorphous, (b) mesomorphous, (c) α form, and (d) β form.

cm^{-1}) and relative absorbances (1.7:1.1:1.0) of the β form. It is also worth noting (Figure 10B) that the band which is at respectively, 902.5, 905.5, and 911 cm^{-1} for the α-form, amorphous, and β-form samples, for the mesomorphic sample is located at 903.5 cm^{-1}, a position intermediate between those observed for the amorphous and α-form samples.

Conclusions

A comparison between the diffraction intensity of an oriented sample of s-PS in the mesomorphic form and the Fourier transforms calculated for different bundles of chains indicates that the mesomorphic form consists of small and imperfect crystals of the α crystalline form. In particular, the best agreement with the diffraction intensity data is obtained for models in which the paracrystalline disorder is assumed only between the triplets of chains, while a complete order is assumed inside the triplets.

The hypothesis of the mesomorphic form consisting of small and imperfect crystals of the α crystalline form is also confirmed by a detailed analysis of the FTIR spectra of a mesomorphic unoriented sample.

Acknowledgment. This work was supported by the Ministero dell'Università e della Ricerca Scientifica e Tecnologica (Italy) and by the Consiglio Nazionale delle Ricerche.

Appendix

Equation 3 contains the sums of exponential terms, which after some algebraic transformation, become

$$\exp\{-2\pi i\xi[r_a\cos(\psi_a-\Phi)-r_b\cos(\psi_b-\Phi)]\} = \exp\{-2\pi i\xi[(r_a\cos\psi_a-r_b\cos\psi_b)\cos\Phi+(r_a\sin\psi_a-r_b\sin\psi_b)\sin\Phi]\} \quad \text{(A-1)}$$

With the introduction of auxiliary variables r_{ab} representing the distance in the xy plane between the ath and bth atoms and ψ_{ab} representing the angle between the vector r_{ab} and the x axis, the exponential term on the right side of eq A-1 can be rewritten as

$$\exp\{-2\pi i\xi[(r_a\cos\psi_a-r_b\cos\psi_b)\cos\Phi+(r_a\sin\psi_a-r_b\sin\psi_b)\sin\Phi]\} = \exp[2\pi i\xi r_{ab}\cos(\psi_{ab}-\Phi)] \quad \text{(A-2)}$$

Hence, the integral of eq 3 over Φ becomes the sum of integrals of the kind

$$\int_0^{2\pi}\exp[2\pi i\xi r_{ab}\cos(\psi_{ab}-\Phi)]d\Phi \quad \text{(A-3)}$$

multiplied by terms which do not depend on Φ. Integrals of this kind have as solution 2π multiplied by the zero-order Bessel function with argument $2\pi\xi r_{ab}$, $J_0(2\pi\xi r_{ab})$.

References and Notes

(1) Ishihara, N.; Seimiya, T.; Kuramoto, M.; Uoi, M. *Macromolecules* **1986**, *19*, 2465.
(2) Zambelli, A.; Longo, P.; Pellecchia, C.; Grassi, A. *Macromolecules* **1987**, *20*, 2035.
(3) Ishihara, N.; Kuramoto, M.; Uoi, M. *Macromolecules* **1988**, *21*, 3356.
(4) Chatani, Y.; Fujii, Y.; Shimane, Y.; Ijitsu, T. *Polym. Prepr., Jpn. (Engl. Ed.)* **1988**, *37*, E428.
(5) Immirzi, A.; De Candia, F.; Iannelli, P.; Vittoria, V.; Zambelli, A. *Makromol. Chem., Rapid Commun.* **1988**, *9*, 761.
(6) Vittoria, V.; De Candia, F.; Iannelli, P.; Immirzi, A. *Makromol. Chem., Rapid Commun.* **1988**, *9*, 765.
(7) Guerra, G.; Vitagliano, V. M.; Corradini, P.; Albizzati, E. Ital. Pat. 19588 (Feb 1989) (Himont, Inc.).
(8) Vittoria, V.; Russo, R.; De Candia, F. *J. Macromol. Sci. Phys.* **1989**, *B28*, 419.
(9) Guerra, G.; Vitagliano, V. M.; De Rosa, C.; Petraccone, V.; Corradini, P. *Macromolecules* **1990**, *23*, 1539.
(10) Guerra, G.; De Rosa, C.; Vitagliano, V. M.; Petraccone, V.; Corradini, P. *J. Polym. Sci., Polym. Phys. Ed.* **1991**, *29*, 265.
(11) Guerra, G.; De Rosa, C.; Vitagliano, V. M.; Petraccone, V.; Corradini, P.; Karasz, F. E. *Polym. Commun.* **1991**, *32*, 30.
(12) De Rosa, C.; Guerra, G.; Petraccone, V.; Corradini, P. *Polym. J.* **1991**, *23*, 1435.
(13) Rapacciuolo, M. T.; De Rosa, C.; Guerra, G.; Mensitieri, G.; Apicella, A.; Del Nobile, M. A. *J. Mater. Sci., Lett.* **1991**, *10*, 1084.
(14) De Rosa, C.; Rapacciuolo, M. T.; Guerra, G.; Petraccone, V.; Corradini, P. *Polymer* **1992**, *33*, 1423.
(15) Chatani, Y.; Shimane, Y.; Inoue, Y.; Inagaki, T.; Ishioka, T.; Ijitsu, T.; Yukinari, T. *Polymer* **1992**, *33*, 488.
(16) Greis, O.; Xu, Y.; Asano, T.; Petermann, J. *Polymer* **1989**, *30*, 590.
(17) Conti, G.; Santoro, E.; Resconi, L.; Zerbi, G. *Mikrochim. Acta* **1988**, *1*, 297.
(18) Niquist, R. A. *Appl. Spectrosc.* **1989**, *43*, 440.
(19) Reynolds, N. M.; Savage, J. D.; Hsu, S. L. *Macromolecules* **1989**, *22*, 2867.
(20) Kobayashi, M.; Nakaoki, T.; Ishihara, N. *Macromolecules* **1990**, *23*, 78.
(21) Guerra, G.; Musto, P.; Karasz, F. E.; MacKnight, W. J. *Makromol. Chem.* **1990**, *191*, 2111.
(22) Vittoria, V. *Polym. Commun.* **1990**, *31*, 263.
(23) Filho, A. R.; Vittoria, V. *Makromol. Chem., Rapid Commun.* **1990**, *11*, 199.
(24) Reynolds, N. M.; Hsu, S. L. *Macromolecules* **1990**, *23*, 3463.
(25) Reynolds, N. M.; Stidham, H. D.; Hsu, S. L. *Macromolecules* **1991**, *24*, 3662.
(26) Grassi, A.; Longo, P.; Guerra, G. *Makromol. Chem., Rapid Commun.* **1989**, *10*, 687.
(27) Gomez, M. A.; Tonelli, A. E. *Macromolecules* **1990**, *23*, 3385.
(28) De Candia, F.; Filho, A. R.; Vittoria, V. *Makromol. Chem., Rapid Commun.* **1991**, *12*, 295.
(29) Petraccone, V.; Auriemma, F.; Dal Poggetto, F.; De Rosa, C.; Guerra, G.; Corradini, P. *Makromol. Chem.* **1993**, *194*, 1335.
(30) Petraccone, V.; De Rosa, C.; Guerra, G.; Iuliano, M.; Corradini, P. *Polymer* **1992**, *33*, 22. Guerra, G.; De Rosa, C.; Juliano, M.; Petraccone, V.; Pucciariello, R.; Villani, V.; Ajroldi, G. *Makromol. Chem.* **1992**, *193*, 549.
(31) Tadokoro, H. *Structure of crystalline polymers*; Wiley: New York, 1979.
(32) James, R. W. *The optical principles of the diffraction of X-ray*; Bell: London, 1962.
(33) Corradini, P.; Napolitano, R.; Pirozzi, V. *Eur. Polym. J.* **1990**, *26*, 157.
(34) Pirozzi, B.; Napolitano, R. Private communication.